THE ASTROPHYSICAL JOURNAL, 283:413–420, 1984 August 1

THREE-DIMENSIONAL STRUCTURES OF TWO SOLAR ACTIVE REGIONS FROM VLA OBSERVATIONS AT 2, 6, AND 20 CENTIMETER WAVELENGTHS

R. K. SHEVGAONKAR[1] AND M. R. KUNDU
Astronomy Program, University of Maryland
Received 1983 October 20; accepted 1984 January 31

ABSTRACT

Three-dimensional structures of two active region groups are determined from observations with the Very Large Array (VLA) at 2, 6, and 20 cm. One of the groups exhibits a single magnetic loop of length $\sim 10^{10}$ cm. The 2 cm radiation is mostly thermal bremsstrahlung and originates from the footpoints of the loop. The 6 and 20 cm radiation is dominated by low-harmonic gyroresonance radiation and originates from the upper portion of the legs or the top of the loop. The loop broadens toward the apex. The top of the loop is not found to be the hottest point, but two temperature maxima on either side of the loop apex are observed, which is consistent with the model proposed for long loops. From 2 and 6 cm observations it can be concluded that the electron density and temperature cannot be uniform in a plane perpendicular to the axis of the loop; the density should decrease away from the axis of the loop.

Subject headings: interferometry — radiation mechanisms — Sun: magnetic fields — Sun: radio radiation

I. INTRODUCTION

The three-dimensional structure of the magnetic fields above active regions in the Sun's chromosphere, corona, and chromosphere-corona transition zone is relatively unknown. This is because the optical methods of determining the magnetic fields in these regions have so far not been very successful, owing to the difficulties of interpreting the spectral lines, and the radio methods have not been exploited fully. Radio methods of measuring magnetic fields in active regions are based upon the measurement of circular polarization and at present are more precise than the optical ones. This is especially true at centimeter wavelengths, where the generating mechanisms of radio emission in active regions are well understood. The generating mechanism of radio waves from active regions is wavelength dependent. Thus, the gyroresonance absorption at the low harmonics of the gyrofrequency is relevant for sunspot-associated active regions at wavelengths lying between about 3 cm and 20 cm, whereas for below and above these limits the free-free process may be appropriate. Both these processes can be used for the measurement of magnetic fields. The circular polarization in the gyroresonance absorption process is due to the fact that for typical conditions in the corona, the extraordinary mode becomes optically thick at the levels where $f = 3f_H$ or $2f_H$ (f_H = gyrofrequency), whereas the ordinary mode becomes optically thick at the level $f = 2f_H$, which is located at a lower level in the Sun's atmosphere; the circular polarization in the extraordinary mode then results as a consequence of the temperature structure above active regions. In the free-free process, the circular polarization results from the fact that in the presence of a magnetic field the absorption coefficient in the extraordinary mode is higher than that in the ordinary mode; consequently, the $\tau = 1$ level in the *e*-mode occurs higher in the solar atmosphere than in the *o*-mode. Both these processes have been used to estimate magnetic field strengths at centimeter and millimeter wavelengths (Alissandrakis, Kundu, and Lantos 1981; Kundu *et al.* 1977; Kundu and McCullough 1972). In any case, as long as there is no radio wave propagation effect in the corona, the circular polarization maps can be used as chromospheric and coronal magnetograms. The absence of such effects can be verified from the correspondence of the radio polarities with those of the photospheric magnetic field.

Aside from the magnetic field structure, the knowledge of the structure of an active region as a function of height is important. This is especially so when the active region appears in the form of a loop, as is often the case at centimeter wavelengths. If the observations are performed at only one or two wavelengths, only a portion of the loop can be observed. Three-dimensional active region studies have been reported by Lang, Willson, and Gaizauskas (1983) and Lang and Willson (1983) from multifrequency observations with the VLA and WSRT. They have used a two-component model of an active region to interpret their results. According to this model the plage-associated active region radiation is due to bremsstrahlung, and the sunspot-associated component could be due to either bremsstrahlung or gyroresonance absorption. Velusamy and Kundu (1981) found that gyroresonance emission is the most likely source of 20 cm radiation from post-flare loops, whereas, in a study of an active region by Lang, Willson, and Rayrole (1982), they attribute the entire 20 cm radiation to bremsstrahlung. McConnell and Kundu (1983) have observed looplike structures at 20 cm, and assuming the theoretical loop model of Rosner, Tucker, and Vaiana (1978), they argue that their observations cannot be explained by thermal bremsstrahlung, and the gyroresonance radiation has to be invoked. All these authors assume that 20 cm radiation comes from optically thick layers, but then it is not consistent with Rosner *et al.*'s model since the 20 cm brightness temperature is less than that at 6 cm.

Here we present multifrequency observations of two active regions. One region exhibits a single loop without any other interacting loop nearby. This region appears to be formed between two strong opposite magnetic poles associated with two different active regions. The observation of this loop at three frequencies not only gives an understanding of the radi-

[1] On leave from Indian Institute of Astrophysics, Bangalore, India.

ation mechanism, but also provides information about the divergence of the magnetic field with height and the temperature variation along the loop. The other region appears in the form of two adjacent and possibly interacting loops.

II. OBSERVATIONS

Three-dimensional studies of the two active regions were performed by observing them at three wavelengths, namely, 20 cm, 6 cm, and 2 cm, using the VLA on 1983 May 1 and 2. Since a nonflaring active region does not change appreciably over a period of an hour, instead of dividing the VLA antennas into three subarrays for simultaneous observations, the entire array was used in a time-sharing mode. Observations were made sequentially at each wavelength for about 8 minutes on the active region and 4 minutes on the calibrator. This sequential observing provided 8 minutes of on-source observation at each frequency for every half-hour of observing. During our observation, the VLA was in C configuration, giving u-v coverage from $\sim$20 m to 3400 m over a 12 hr period. The receiver bandwidth selected was 12.5 MHz.

On the two days of observing there were two active region groups. Group A, consisting of three active regions, AR 4154, AR 4157, and AR 4162, was located in the western hemisphere. The other region B, consisting of AR 4165, was in the eastern hemisphere, and on the first day was situated at 60°E heliographic longitude, which was not a suitable location for our purpose. Therefore, on the first day, only region A was observed. The primary beam of the antenna was centered at S14W24 at 00 hours IAT on that day. For the first half of the second day, region B was observed, and during the second half, region A was observed again for about 4 hr.

Omitting the data during which some minor flares occurred, the entire day's visibility data were used to produce the active region maps. The standard CLEAN technique was applied to make the maps free from unwanted sidelobe responses. The final resolution in the CLEANed maps was 20″, 5″, and 2″ at 20 cm, 6 cm, and 2 cm, respectively.

III. RESULTS

As mentioned above, two active region groups, A and B, were observed at three wavelengths. Group A consists of three active regions, which were all covered within the primary beam at 20 cm. At 6 cm and 2 cm, however, only two regions, AR 4154 and AR 4157, were inside the primary beam; the region AR 4162 was outside the half-power points of the beam.

a) Group A

Figures 1–3 show the total intensity (I) and circular polarization (V) maps at the three wavelengths. The beam, maximum brightness temperature, and the contour levels are indicated on the maps. Figure 4 (Plate 7) shows the superposition of the 2 cm map over the magnetogram. The 2 cm radiation coming from two isolated spots has a brightness temperature of $\sim 1.5 \times 10^5$ K. These two isolated regions are cospatial with two strong magnetic regions with opposite polarities. Both regions are very highly polarized, $\sim$80%. The sense of polarization for the two regions is opposite and has the same sign as the magnetic fields on the magnetogram. From the I and V maps it is clear that the 2 cm radiation appears from the footpoints of a magnetic loop. The 6 cm total intensity map again shows two regions, more or less at the same positions as the 2 cm regions, but larger in size. The brightness temperature at 6 cm is as high as 4.5×10^6 K, and the degree of polarization falls off to almost the detection limit, i.e., $\sim$10%–15%. The larger size of the two regions at 6 cm compared with that at 2 cm indicates that, if the active region emission originates in a loop, the loop must be diverging toward its apex. The existence of two isolated regions at 6 cm, having temperatures of $\sim 4.5 \times 10^6$ K, indicates that the two legs of the loop have not started closing, and that the 6 cm radiation originates from the upper part of

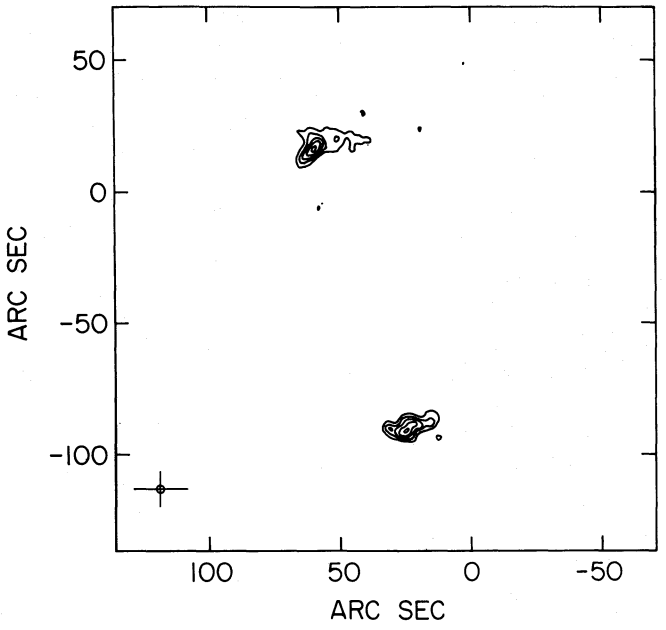

FIG. 1a

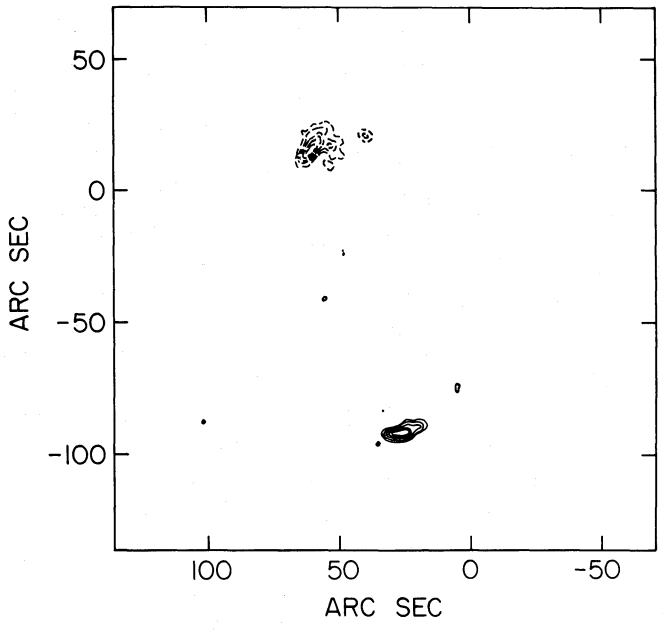

FIG. 1b

FIG. 1.—Group A active region synthesized maps at 2 cm. (*a*) Total intensity (I) map; peak $T_B = 1.50 \times 10^5$ K, contour interval = 2.90×10^4 K. (*b*) Circular polarization (V) map; peak $T_B = 1.15 \times 10^5$ K, contour interval = 1.94×10^4 K.

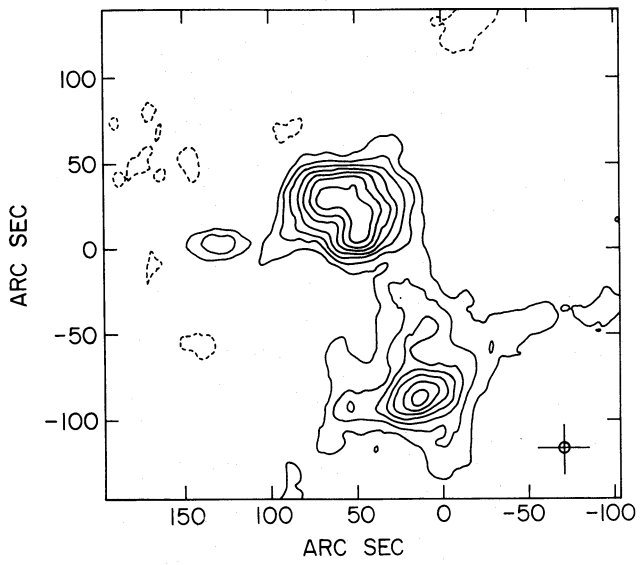

FIG. 2a

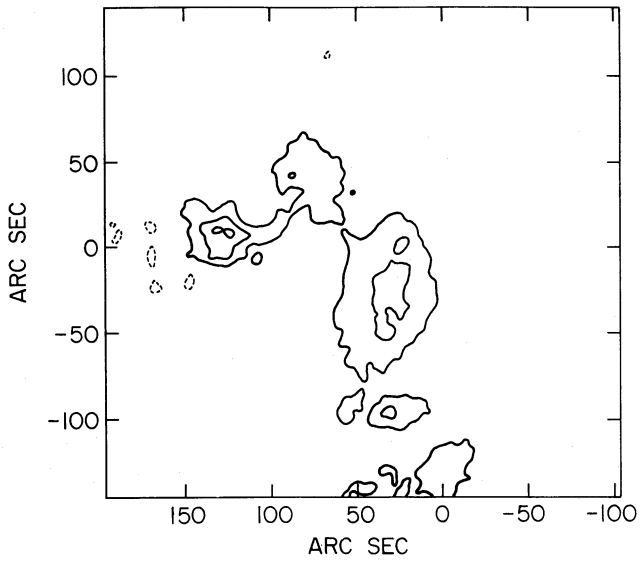

FIG. 2b

FIG. 2.—Group A active region synthesized maps at 6 cm. (*a*) *I* map; peak $T_B = 4.59 \times 10^6$ K, contour interval = 5.88×10^5 K. (*b*) *V* map; peak $T_B = 0.71 \times 10^6$ K, contour interval = 2.20×10^5 K.

the legs of the loop. It seems that at 20 cm, the two regions are almost merged into each other but still keep their identity as two regions. The centers of these two merging regions are again cospatial with the 6 cm peaks within the errors of measurement. The size of the two 20 cm regions is larger than that at 6 cm, but the peak brightness temperature has decreased to $\sim 2.5 \times 10^6$ K. The polarization is again small, $\sim 20\%$. At 20 cm, a third region shows up in the upper right corner of the map, coinciding with a magnetic arcade seen in the magnetogram (Fig. 5 [Pl. 7]).

Comparison of the maps over a period of two days (Figs. 3 and 6 [Pl. 8]) show that the structure of the regions at 20 cm has not changed, except that a small source appeared on the second day just above the double-peaked region of Figure 3*a*. This source is coincident in position with a small evolving magnetic region observed in the magnetogram.

b) Group B

The region in group B is much more complex in magnetic structure than the regions in group A. The 2 cm map (Fig. 7) appears rather patchy in contrast to the two simple isolated regions of group A, which must be the footpoints of a loop. Also, unlike the group A loop, the brightness temperatures in this region are rather low, $\sim 5 \times 10^4$ K, and it does not exhibit any significant polarization. The 2 cm map does not show much correlation with the magnetogram. The 6 cm map (Fig.

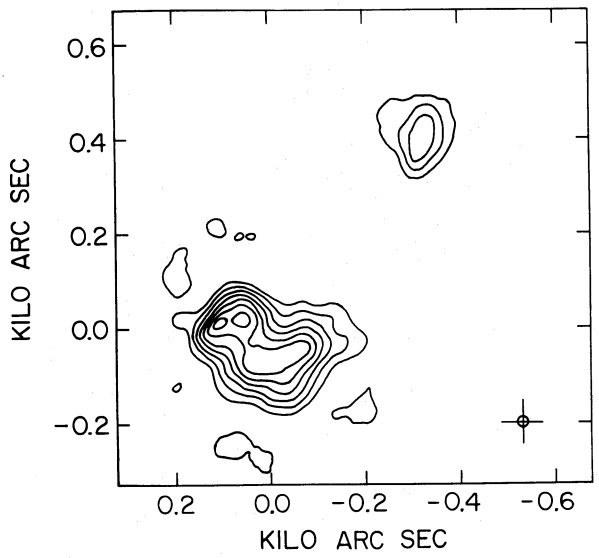

FIG. 3a

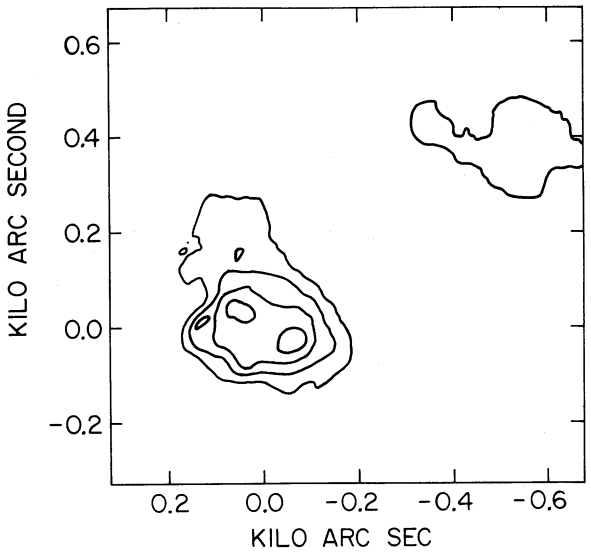

FIG. 3b

FIG. 3.—Group A active region synthesized maps at 20 cm. (*a*) *I* map; peak $T_B = 2.32 \times 10^6$ K, contour interval = 3.12×10^5 K. (*b*) *V* map; peak $T_B = 0.49 \times 10^6$ K, contour interval = 1.04×10^5 K.

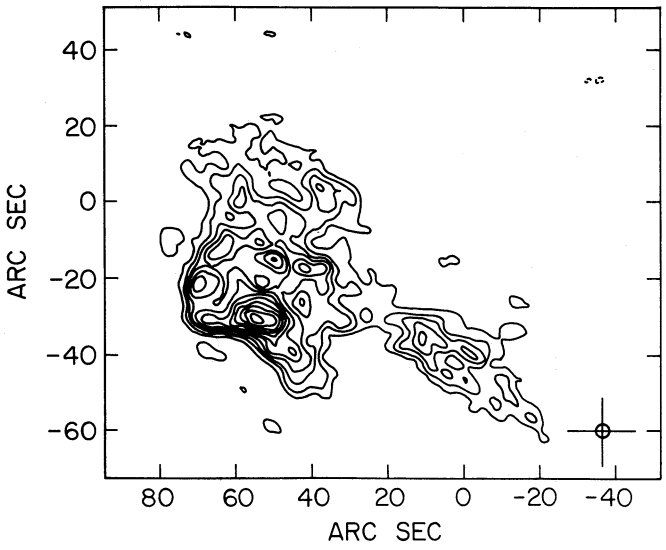

FIG. 7a

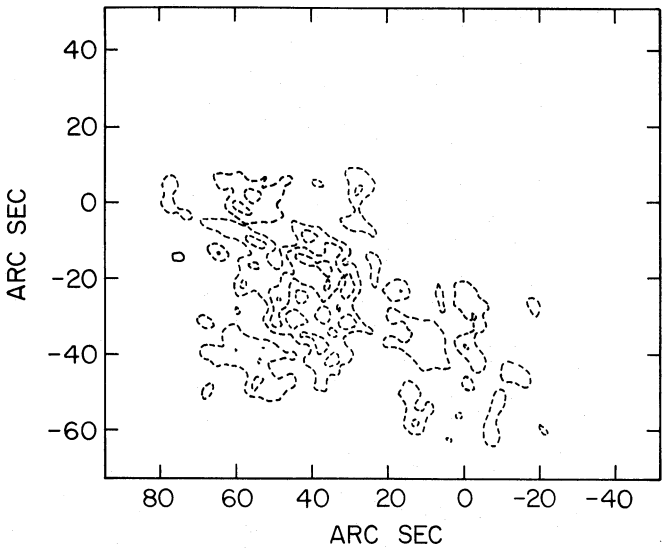

FIG. 7b

FIG. 7.—Group B active region synthesized maps at 2 cm. (*a*) *I* map; peak $T_B = 0.49 \times 10^5$ K, contour interval = 0.43×10^4 K. (*b*) *V* map; peak $T_B = -0.06 \times 10^5$ K, contour interval = 0.172×10^4 K.

8) shows four peaks, B1, B2, B3, B4, and a faint bridge joining B2 and B3. These four peaks coincide very well spatially with strong magnetic regions in the magnetogram (Fig. 8*c*). The *V* map has two peaks cospatial with the two peaks B1 and B2 in the corresponding *I* map. Both peaks are about ~30% polarized and have the same sense of circular polarization. From Figure 8, one can visualize the existence of two magnetic loops, one loop joining peaks B1 and B3 and another loop joining peaks B2 and B4, approximately parallel to each other. The peak brightness temperature at 6 cm is $\sim 4.5 \times 10^6$ K. The 20 cm map shown in Figure 9 has three peaks. The middle broad peak corresponds to the loop structure shown in the corresponding 6 cm map. The peak brightness temperature for the middle source is $\sim 3 \times 10^6$ K, and the degree of polarization is ~15%. The peak located on the right side of the map is in good positional agreement with the negative magnetic region seen in the magnetogram (Fig. 10 [Pl. 9]). Its peak brightness temperature is $\sim 1.2 \times 10^6$ K, and it has a higher degree of polarization, ~50%. This peak has not been mapped at 6 cm or 2 cm, as it falls outside the primary beam at these wave-

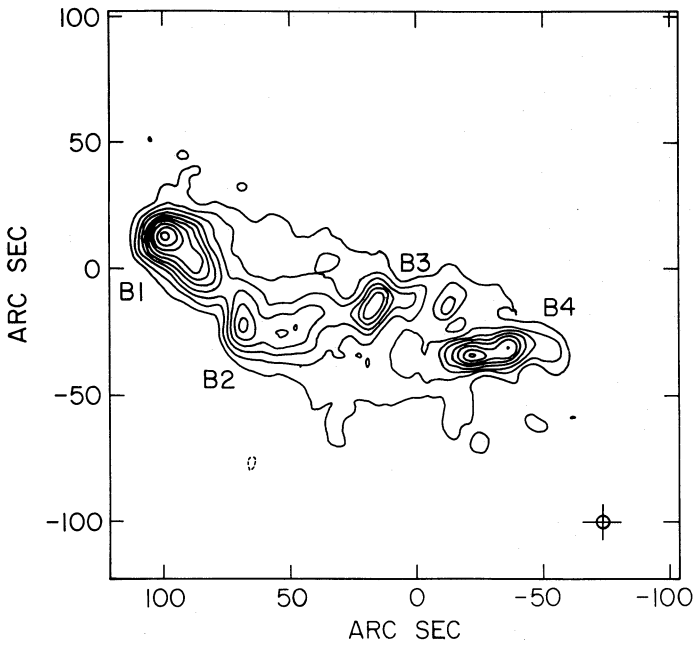

FIG. 8a

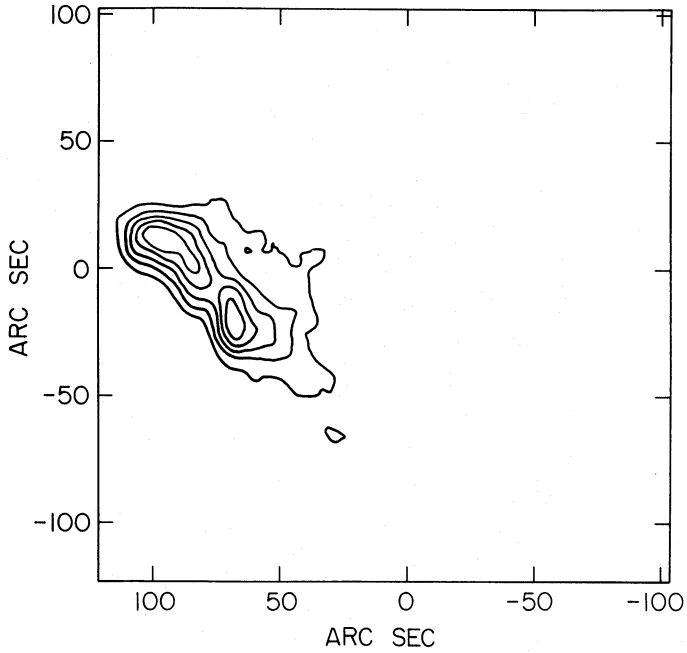

FIG. 8b

FIG. 8.—Group B active region synthesized maps at 6 cm. (*a*) *I* map; peak $T_B = 4.63 \times 10^6$ K, contour interval = 4.41×10^6 K. (*b*) *V* map; peak $T_B = 1.32 \times 10^6$ K, contour interval = 2.20×10^5 K.

FIG. 8*c*.—Group B *I* map at 6 cm superposed on the magnetogram

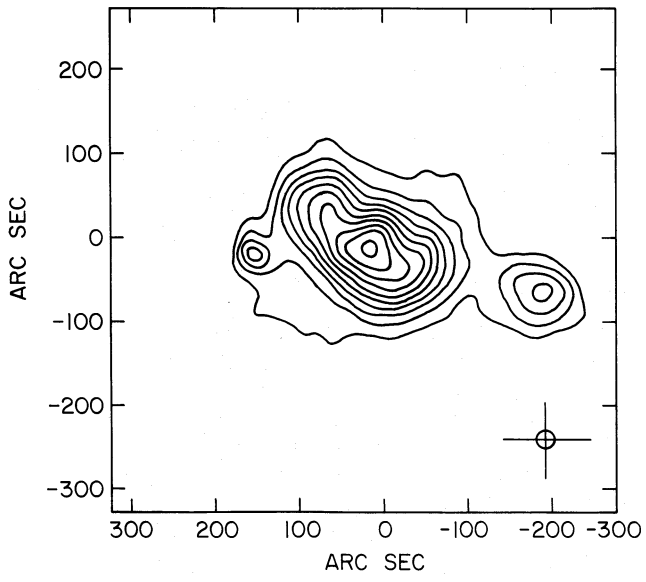

FIG. 9a

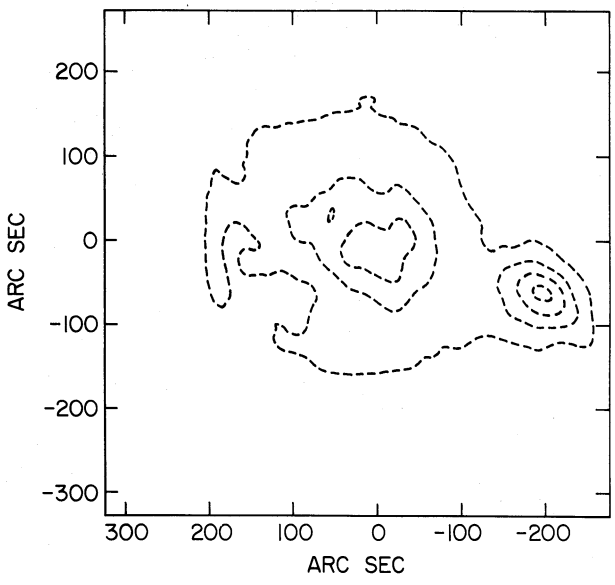

FIG. 9b

FIG. 9.—Group B active region synthesized maps at 20 cm. (*a*) *I* map; contour interval = 0.31×10^6 K. (*b*) *V* map; peak $T_B = -0.66 \times 10^6$ K, contour interval = 1.56×10^5 K.

lengths. The middle peak obviously corresponds to the radiation coming from the top of the loops, visible in the 6 cm map (Fig. 8).

IV. DISCUSSION

a) Group A

From Figures 1–3, it is apparent that the maps give sectional views of a magnetic loop at different heights. The magnetic field diverges along the loop in the upward direction. The loop seems to start closing at a height of approximately 50×10^3 km, where the 20 cm radiation originates (Lang and Willson 1983; Felli, Lang, and Willson 1981). The two isolated compact regions observed at 2 cm are cospatial with two sunspots having opposite magnetic polarities. The degree of polarization is high, and comparison with the magnetogram indicates that the radiation is emitted in the extraordinary mode. This means that the extraordinary mode is optically thick in the transition zone where the temperature is $\sim 1.5 \times 10^5$ K, and the ordinary mode becomes optically thick at a lower level (i.e., for a lower harmonic) where the temperature is less than $\sim 10^5$ K or it is optically thin.

The active region emission at 2 cm is believed to be due to either thermal bremsstrahlung or gyroresonance radiation. The optical depths in the two cases are given by (Zheleznyakov 1970)

$$\tau_{\rm br} \approx \frac{7N_e^2 L}{\omega^2 T_e^{3/2}[1 \mp (\omega_H |\cos\alpha|)/\omega]^2}, \quad (1)$$

$$\tau_{\rm res} \approx \frac{\pi s^{2s}}{2^{s+1} s!} \frac{3.18 \times 10^9 N_e}{\omega c} \times (1.77 \times 10^{-10} T_e)^{s-1} L_H (1 \pm \cos\alpha)^2 \sin^{2s-2}\alpha, \quad (2)$$

where N_e = electron density, ω = angular frequency, T_e = electron temperature of the radiating layer, ω_H = electron gyrofrequency, L = thickness of the radiating layer, L_H = scale height of magnetic field, s = harmonic number, c = velocity of light, α = angle between the line of sight and the direction of the magnetic field.

Taking $\alpha \approx 30° \approx$ longitude of the active region, and typical values for the other parameters (e.g., $L \sim 5 \times 10^8$ cm, $L_H \sim 10^9$ cm, $T_e \sim 1.5 \times 10^5$ K), for 2 cm thermal bremsstrahlung radiation to be optically thick, $N_e \sim 10^{10}$ cm^{-3}, which is a reasonable estimate. The observed high degree of polarization requires the resonance frequency of the radiating layer to be $\omega_H \sim \omega/2.3$, which implies a magnetic field strength of ~ 2200 G in the radiating layer. On the other hand, if the emission is due to gyroresonance absorption, and we consider $s = 2$, for the extraordinary mode to be optically thick and the ordinary mode to be optically thin, $N_e \sim 5 \times 10^8$ cm^{-3}, which is too low. If we take a more reasonable value for N_e of $\sim 10^{10}$ cm^{-3}, both modes become optically thick ($\tau_e \approx 200$ and $\tau_o \approx 1$), and the observed polarization cannot be explained. For $s = 3$ and $N_e = 10^{10}$ cm^{-3}, both waves are optically thin; $\tau_e \approx 0.04$, $\tau_o \approx 2 \times 10^{-4}$. The observation can be explained if the 2 cm radiation is dominated by thermal bremsstrahlung and originates from a layer where $N_e \sim 10^{10}$ cm^{-3} and $B \sim 2000$ G. Alternately, one can explain the radiation if $N_e = 10^{11}$ and $s = 3$.

The brightness temperatures at 6 cm are $\sim 4.5 \times 10^6$ K, and the polarization is $\sim 15\%$. Because of the small percentage polarization, either of the radiation mechanisms can be considered. For bremsstrahlung radiation to be optically thick ($\tau \approx 1$), the electron density required is $\sim 2 \times 10^{10}$ cm^{-3}, which is much higher than what we expect at a height of $\sim 10^4$ km. Because the observed polarization is $\sim 15\%$, $\tau_e > 1$ and $\tau_o \sim 1$. Taking $\alpha \approx 45°$, $L_H = 10^9$ cm, $N_e = 4 \times 10^9$ cm^{-3}, the highest harmonic for which both modes are optically thick is 3, resulting in a magnetic field strength of ~ 600 G at a height of $\sim 10^4$ km. If the same magnetic field which produces the required polarized emission at 2 cm also generates the 6 cm gyroresonance emission, the conservation of the magnetic flux requires that the decrease in the magnetic field due to its divergence should be inversely proportional to the magnetic loop cross-sectional area. So, if the magnetic field at 6 cm level is

TABLE 1

OBSERVED PARAMETERS OF GROUP A ACTIVE REGION

Wavelength (cm)	Peak T_B (K)	% Polarization	Average Source Size
2.0.....	1.52×10^5	80	15″ × 10″
6.0.....	4.59×10^6	~15	60″ × 60″
20.0.....	2.32×10^6	20–25	150″ × 120″

~600 G and at 2 cm level ~2200 G, the ratio of the source sizes at 6 cm and 2 cm should be ~3.5. But from Table 1, the ratio is ~24. This discrepancy cannot be removed if we assume that loop parameters such as the temperature and electron density are constant in the radial direction of the loop. Comparison of the 2 cm map and the magnetogram shows that the two 2 cm regions lie within two magnetic poles. The reduction of the brightness temperature in the outer rims of the magnetic poles requires the rims to be optically thin, which in turn requires an increase in T_e, or a reduction in N_e, or both (assuming 2 cm radiation to be due to thermal bremsstrahlung). From equation (1),

$$\tau_{\rm br} \propto N_e^2 T_e^{-3/2} . \quad (3)$$

The pressure inside the loop is given by

$$p \propto N_e T_e . \quad (4)$$

For the loop to be in hydrostatic equilibrium,

$$B^2 \propto N_e T_e . \quad (5)$$

Now, since the emission in the outer rim of the magnetic pole is less than 10% of its peak value, the optical depth should be $\gtrsim 0.1$. If we take the optical depth in the core to be ~1 (i.e., the region is marginally optically thick), since $T_B \propto N_e^2 T_e^{-1/2}$ (for an optically thin region), for T_B in the outer rim to be $\leq 10\%$ of that in the core, either the N_e should decrease by a factor of ~3 or T_e has to increase by a factor of ~100. Even if a cool-core magnetic loop model is assumed, the increase by a factor of 100 is quite high. Also, if the temperature in the outer rim is two orders of magnitude higher than that in the core, the gyroresonance will make the outer rim optically thick, and the observations cannot be explained. Thus, a reduction in N_e looks more plausible. Considering the hydrostatic equilibrium of the loop, for a reduction in N_e by a factor of 3, the magnetic field will decrease toward the edge of the loop by a factor of 1.76 if T_e is taken constant or even more slowly if a cool-core model is assumed, which in fact is quite consistent with combined high-resolution microwave and soft X-ray observations (Strong, Alissandrakis, and Kundu 1984). Assuming that the magnetic field remains more or less constant over the outer rim, the conservation of flux gives a size of the magnetic pole which is ~2.5 times that of the 2 cm region and is the same as the size of the pole in the magnetogram.

At 20 cm, the radiation originates from the upper portion of the legs of the loop. The brightness temperature is $\sim 2.5 \times 10^6$ K, and the degree of polarization ~20%. According to the loop model with uniform energy deposition function along the loop as suggested by Rosner, Tucker, and Vaiana (1978), the loop apex is hottest, and so T_B at 20 cm level must be at least 5×10^6 K, the same as the 6 cm T_B. But since the observed T_B is $\sim 2.5 \times 10^6$ K, the radiation must be optically thin, with $\tau \sim 0.7$, to satisfy the Rosner *et al.*'s model. For a source of dimension 5×10^9 cm, the N_e required to allow $\tau \sim 0.7$ due to thermal bremsstrahlung should be $\sim 4 \times 10^9$ cm^{-3}, i.e., an emission measure of $\sim 10^{29}$ cm^{-5}. This emission measure is higher by about one order of magnitude than that computed by Lang, Willson, and Gaizauskas (1983) from VLA observations and by Vaiana and Rosner (1979) from X-ray observations. Even if this value of N_e is permitted, one should check the contribution due to gyroresonance absorption. From magnetic flux conservation, the source size at 20 cm compared with that at 6 cm gives a magnetic field of ~150 G at 20 cm level, which is sufficient to generate the third or fourth harmonic emission at 20 cm. Near the apex of the loop, where the field lines start closing, taking $\alpha \sim 75°$ and $N_e \sim 4 \times 10^9$ cm^{-3} (required to give $\tau = 0.7$ for thermal bremsstrahlung), $\tau_{\rm res}$ for both modes is $\gg 1$ for $s = 4$ ($\tau_e = 12$ and $\tau_o = 4$) (i.e., both modes are optically thick) and $\ll 1$ for $s = 5$. It is clear that for this situation the gyroresonance absorption dominates over bremsstrahlung, and the 20 cm radiation must be due to gyroresonance only. The same conclusion was reached by McConnell and Kundu (1983). For $s = 3$, $\tau_{\rm res} \sim 10^3$ for both modes. By reducing the electron density N_e, which is a free parameter, it does not seem that the radiation can be made optically thin for $s = 3$. Thus, T_e must be 2.5×10^6 K. It can be seen that for an emission measure of $\sim 10^{28}$ cm^{-5}, i.e., $N_e \sim 10^9$ cm^{-3}, the region is optically thin due to thermal bremsstrahlung for temperatures ranging from 2×10^6 to 5×10^6 K, and the observed high brightness temperature of 2.5×10^6 K cannot be explained by this mechanism. Lang, Willson, and Gaizauskas (1983) conclude from their VLA observations that the 20 cm radiation is optically thin bremsstrahlung. In their observation T_B is $\sim 0.5 \times 10^6$ K at 20 cm, and the bremsstrahlung opacity is adequate to produce the observed T_B for an electron temperature $\sim 2 \times 10^6$ K. However, to get $T_B \sim 2.5 \times 10^6$ K as observed by us, the gyroresonance mechanism has to be invoked. The above arguments show that the higher layer from which the 20 cm radiation originates is cooler than the lower layer from which the 6 cm radiation originates. This result does not support Rosner *et al.*'s model of uniform energy deposition along the loop, which gives maximum temperature at the apex of the loop. On the contrary, our observations provide evidence for Vesecky, Antiochos, and Underwood's (1979) model, according to which the temperature maximum need not necessarily occur at the apex of the loop, but there could be two maxima, one on either side of it, and a minimum at the apex of the loop. In a later publication Serio *et al.* (1981) have suggested that for long loops of length $\sim 10^{10}$ cm, the pressure scale height is smaller than the loop height, and the energy deposition function is not uniform. In such a situation there should be a temperature minimum at the apex of the loop.

b) *Group B*

Figures 7–9 again show a three-dimensional view of an active region. Unlike the group A magnetic loop at 2 cm, this region shows a lower T_B of $\sim 0.5 \times 10^5$ K and practically no polarization. Although the 2 cm map overlaps the magnetogram very well, there is no striking correlation between the two. This might indicate that the radiation is not very magnetic field dependent but depends mainly upon temperature and electron density; i.e., the radiation is mostly thermal bremsstrahlung. We shall consider this argument quantitatively.

Assuming the plasma parameters for the radiating layer to be $T_e \sim 0.5 \times 10^5$ K, $N_e \sim 10^{10}$ cm^{-3}, and $L \sim 5 \times 10^8$ cm, the optical depth due to thermal bremsstrahlung $\tau_{\rm br}$ is ~4; i.e., the layer is optically thick. On the other hand, the optical

depth due to gyroresonance for $s = 3$ is $\sim 10^{-2}$ for the same parameters. Like the group A active region, the radiation at 2 cm in this region also is mostly dominated by thermal bremsstrahlung; the lack of high polarization in this case is probably due to weaker magnetic fields.

The 6 cm map shown in Figure 8 clearly exhibits two loops which are more or less parallel to each other. The brightness temperatures in both loops are again $\sim 4.5 \times 10^6$ K, but only one leg of each loop shows polarization, $\sim 30\%$. A superposition of the 6 cm map on the magnetogram is shown in Figure 8*c*. Following the same arguments as for group A, the radiation can be attributed to gyroresonance absorption. The presence of polarization in only one leg of each loop is expected if we consider the geometry and the location of the active region on the solar disk. For the observed orientation of the loops, which are more or less parallel to the solar equator and at heliographic longitude $\sim 40°$, the field lines make a small angle with the line of sight at peaks B1 and B2; thus, the two intense peaks could be marginally optically thick for the extraordinary mode and therefore optically thin for the ordinary mode, resulting in the observed polarization. On the other hand, at 6 cm level the magnetic field over the other two peaks, B3 and B4, makes a much larger angle with the line of sight, thus rendering both modes optically thick, with the result that no polarization is observed.

Considering the 20 cm map, it is clear that unlike the radiation from the loop in group A, the radiation does not originate from the upper portion of the legs of the loop but from the top of the loop. From similar arguments made earlier (for group A) and also from the arguments presented by McConnell and Kundu (1983), the peak brightness temperature at the loop top can be explained by only gyroresonance absorption. According to McConnell and Kundu (1983), the apex of the loop is optically thick for gyroresonance absorption, and the plasma temperature at the loop top, $\sim 3 \times 10^6$ K, is again less than the 6 cm T_B of 4.5×10^6 K.

The peak seen on the right-hand side of the 20 cm map aligns with a unipolar region of negative polarity in the magnetogram (Fig. 10). This region has a T_B of $\sim 1.2 \times 10^6$ K and a degree of polarization of $\sim 50\%$, which can be interpreted as due to the gyroresonance mechanism.

V. CONCLUSIONS

The observations presented in this paper show a three-dimensional picture of a magnetic loop. From the above discussion the following conclusions can be drawn:

1. Radiation at 2 cm is dominated by thermal bremsstrahlung even in the case where the observed degree of polarization is very high, $\sim 80\%$. The presence of a high degree of polarization depends upon the strength of the magnetic field in the radiating layer.
2. The radiation at 6 cm is always due to optically thick gyroresonance absorption, whereas 20 cm radiation could be either due to gyroresonance absorption or due to optically thin thermal bremsstrahlung, depending upon the observed brightness temperature. If T_B is $\lesssim 10^6$ K, the thermal bremsstrahlung mechanism dominates, but for $T_B \gtrsim 2 \times 10^6$ K, the radiation is due to gyroresonance absorption.
3. Since the brightness temperature at 20 cm is less than that at 6 cm and the radiation is optically thick at both wavelengths, the apex of the magnetic loop is not the hottest part of the loop, but two temperature maxima, one on either side of the apex, probably occur. This supports the argument put forward by Vesecky *et al.* that, from thermal stability considerations, there is no reason to expect a temperature maximum at the apex of the loop. This suggests that as the loop length is $\sim 7 \times 10^9$ cm, the pressure scale height is much smaller than the loop length; in such a situation, according to Serio *et al.*, the energy deposition function is not uniform along the loop, and there should be a minimum at the apex of the loop.
4. The constant–cross section loop model assumed by Rosner *et al.* is not very realistic since the loop broadens toward the apex.
5. The 2 cm radiation originates from the core of a magnetic pole. The small value of the brightness temperature in the outer rim of the pole requires that the temperature increase or the density decrease in the radial direction away from the axis of the loop, but a fall in density is more plausible for interpreting the observations. Along with a decrease in the density toward the edge of the loop, a cool core structure may also exist.

We are grateful to Dr. G. D. Holman for a critical reading of the manuscript. We are also thankful to Dr. J. A. Harvey for supplying the magnetograms. The National Radio Astronomy Observatory is operated by Associated Universities, Inc., under contract with the National Science Foundation. This research was supported by NSF grant ATM 8103089, NASA grant NGR 21-002-199, and NASA contract NSG 5320.

REFERENCES

Alissandrakis, C. E., Kundu, M. R., and Lantos, P. 1981, *Astr. Ap.*, **82**, 30.
Felli, M., Lang, K. R., and Willson, R. F. 1981, *Ap. J.*, **247**, 325.
Kundu, M. R., Alissandrakis, C. E., Bregman, J. D., and Hin, A. C. 1977, *Ap. J.*, **213**, 278.
Kundu, M. R., and McCullough, T. P. 1972, *Solar Phys.*, **27**, 182.
Lang, K. R., and Willson, R. F. 1983, in *Solar Maximum Year: Proceedings of Symposium 7 of the COSPAR Twenty-fourth Plenary Meeting Held in Ottawa, Canada, 16th May–2nd June 1982*, ed. Z. Švestka, D. M. Rust, and M. Dryer (*Adv. Space Res.*, Vol. **2**, No. 11), p. 91.
Lang, K. R., Willson, R. F., and Gaizauskas, V. 1983, *Ap. J.*, **267**, 455.
Lang, K. R., Willson, R. F., and Rayrole, J. 1982, *Ap. J.*, **258**, 384.
McConnell, D., and Kundu, M. R. 1983, *Ap. J.*, **269**, 698.
Rosner, R., Tucker, W. H., and Vaiana, G. S. 1978, *Ap. J.*, **220**, 643.
Serio, S., Peres, G., Vaiana, G. S., Golub, L., and Rosner, R. 1981, *Ap. J.*, **243**, 288.
Strong, K. T., Alissandrakis, C. E., and Kundu, M. R. 1984, *Ap. J.*, **277**, 865.
Vaiana, G. S., and Rosner, R. 1978, *Ann. Rev. Astr. Ap.*, **16**, 393.
Velusamy, T., and Kundu, M. R. 1981, *Ap. J. (Letters)*, **243**, L103.
Vesecky, J. F., Antiochos, S. K., and Underwood, J. H. 1979, *Ap. J.*, **233**, 987.
Zheleznyakov, V. V. 1970, *Radio Emission of the Sun and the Planets* (New York: Pergamon), chap. 8.

M. R. KUNDU and R. K. SHEVGAONKAR: Astronomy Program, University of Maryland, College Park, MD 20742

1984ApJ...283..413S

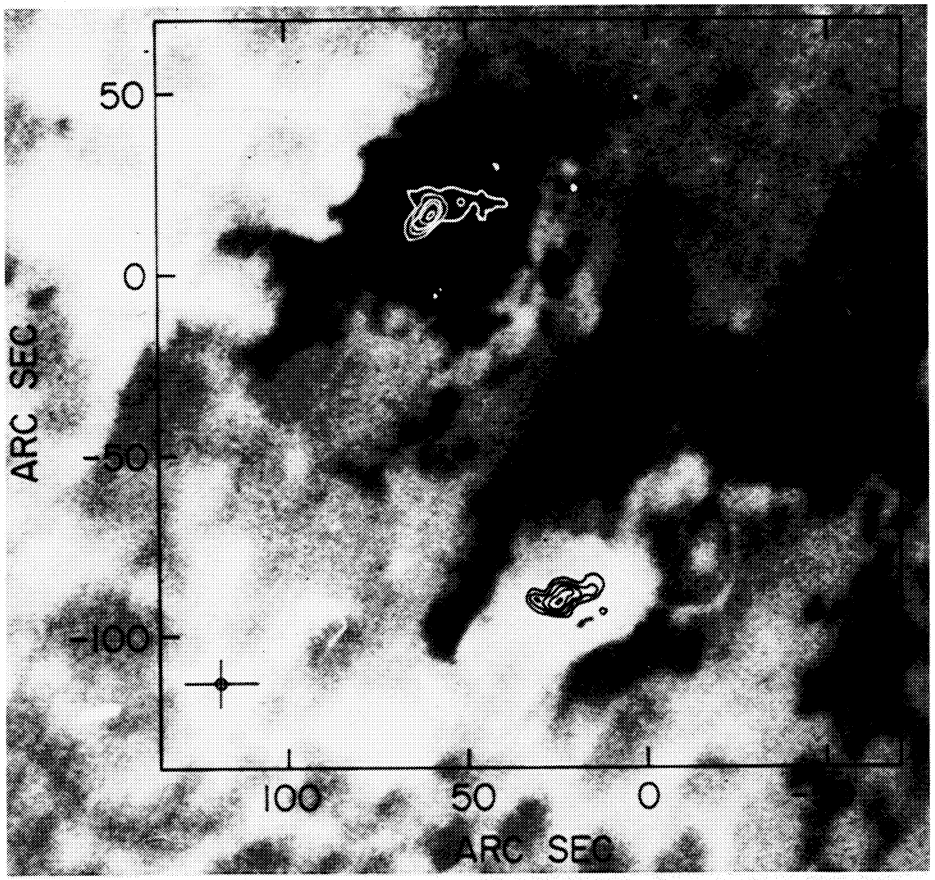

FIG. 4

FIG. 5

FIG. 4.—Group A active region *I* map at 2 cm superposed on the corresponding KPNO magnetogram

FIG. 5.—KPNO magnetogram of the group A active regions observed on 1983 May 1. A1 corresponds to the magnetic loop observed at all three frequencies; A2 is the evolving magnetic region; A3 is the magnetic arcade observed at 20 cm.

SHEVGAONKAR AND KUNDU (*see* pages 414 and 415)

PLATE 8

FIG. 6.—Superposition of the magnetogram and group A active region *I* map at 20 cm observed on 1983 May 2

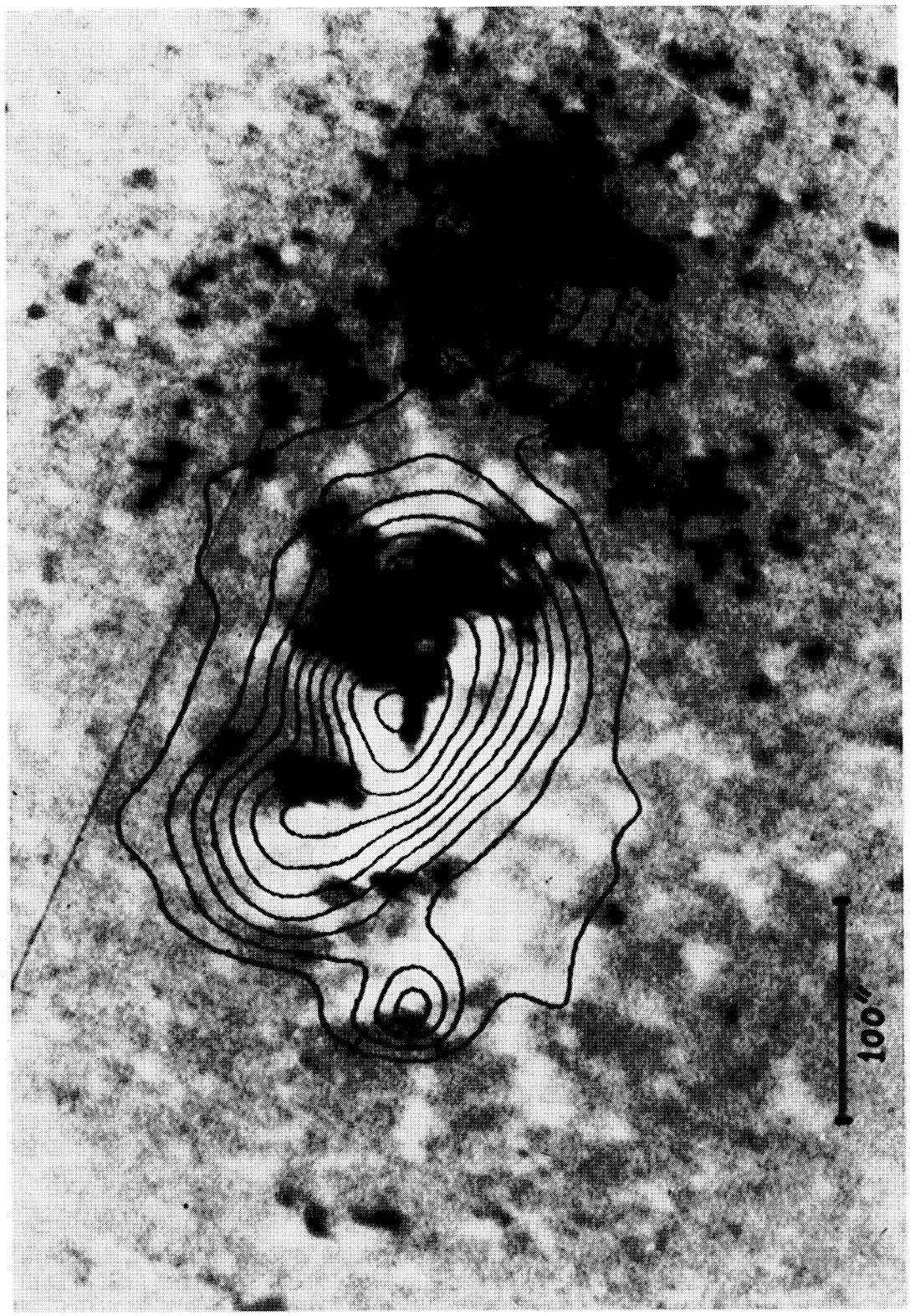

FIG. 10.—Superposition of the magnetogram and the group B active region *I* map at 20 cm